

Pressure effects on the equilibrium configurations of bilayer lipid membranes*

Raffaella De Vita¹, Iain W Stewart^{2,3} and Donald J Leo⁴

¹ Department of Engineering Science and Mechanics, Virginia Tech, 305 Norris Hall, Blacksburg, VA 24061, USA

² Department of Mathematics, Livingstone Tower, 26 Richmond Street, Glasgow G1 1XH, UK

³ Department of Mathematics, University of Strathclyde, Livingstone Tower, 26 Richmond Street, Glasgow G1 1XH, UK

⁴ Center for Intelligent Material Systems and Structures, Department of Mechanical Engineering, Virginia Tech, 310 Durham Hall, Blacksburg, VA, 24061, USA

E-mail: devita@vt.edu

Received 12 April 2007, in final form 13 September 2007

Published 9 October 2007

Online at stacks.iop.org/JPhysA/40/13179

Abstract

Planar bilayer lipid membranes (BLMs) are currently employed to construct many bio-inspired material systems and structures. In order to characterize the pressure effects on the equilibrium configurations of these biological membranes, a novel continuum model is proposed. The BLM is assumed to be a two-layer smectic A liquid crystal. The mean orientation of the amphiphilic molecules comprising the membrane is postulated to be perpendicular to the layers and each layer is idealized as a two-dimensional liquid. Moreover, the BLM is modeled as a simply supported plate undergoing small deformations. It is subjected to a pressure load that acts perpendicularly to the layers. The equilibrium equations and boundary conditions are derived from the bulk elastic energy for smectic A liquid crystals as described by de Gennes and Prost (1993 *The Physics of Liquid Crystals* 2nd edn (Oxford Science Publications)) by using variational methods. The resulting fourth-order linear partial differential equation is solved by employing cylindrical functions and the series solution is proved to be convergent. The solution is numerically computed for values of the model parameters that are reported in the literature.

PACS number: 61.30.Cz

1. Introduction

Bilayer lipid membranes constitute the dominant component of cellular membranes. They help in confining the interior of cells, enclosing their organelles, and mediating the transport

* This paper is dedicated to the memory of our colleagues, Professors Kevin P Granata and Liviu Librescu, who lost their lives during the senseless tragedy on 16 April, 2007 at Virginia Tech.

of molecules into and out of cells and organelles. Their building blocks are amphiphilic molecules. These molecules are characterized by having hydrophilic head groups and hydrophobic tails. Therefore, when a specific concentration of lipid molecules is dissolved in an aqueous medium, planar bilayer lipid membranes (BLMs) are generated in which the hydrophilic heads become exposed to the watery solution whereas the hydrophobic tails constitute the core of the membranes (Alberts *et al* 2002).

Interest in research on BLMs is growing not only because they are the perfect model for studying the cellular membranes but also because they continue to demonstrate their potential use in numerous applications ranging from drug delivery systems (Raviv *et al* 2005, Fang *et al* 2006) to biosensors for detecting biological agents (Sackmann 1996, Cremer and Yang 1999). The BLMs together with sucrose transporters are being employed by the authors to engineer a micro-hydraulic actuator that uses the transport phenomenon occurring at the cellular level to convert biochemical energy into mechanical energy (Sundaresan and Leo 2005). The actual use of BLMs is, however, hampered by their poor stability to environmental disturbances such as, for example, air exposure, contamination, temperature changes, and mechanical stresses.

In order to improve the mechanical performance of bio-material systems and structures which incorporate BLMs, a rigorous investigation of their resistance to various pressure loads is needed. Toward this end, experiments are being conducted by the authors in which the BLMs are reconstituted over porous membranes and, subsequently, pressurized (Hopkinson *et al* 2006, Hopkinson and Leo 2007). Because performing experiments on BLMs is challenging due to the small stresses and deformations involved, the formulation of reliable mathematical models becomes important for designing the experiments and interpreting their results.

Continuum models, which are used to synthesize the experimental findings obtained by using atomic force microscope and micropipette aspiration techniques, are based on the simplifying assumption that the BLMs behave either as solids or fluids. These models include linear elastic and viscoelastic solid models—Newtonian, Maxwell and shear thinning liquid drop models. However, BLMs have been universally recognized to be smectic A liquid crystals (Collings and Hird 1997).

Liquid crystals are mesomorphic states of matter that possess properties that are intermediate between those of crystalline solids and amorphous liquids. In crystalline solids, the molecules are fixed over a lattice with their axes oriented in specific directions whereas, in amorphous liquids, the molecules move randomly in the container they occupy. In liquid crystals, the molecules are free to move although they preserve orientational order. The word smectic comes from the Greek word that means ‘soap-like’. As in soaps, the molecules in smectic liquid crystals form layered structures with defined interlayer spacing exhibiting both orientational and positional order. Specifically, the molecular axes in smectic A liquid crystals are normal to the layers. Layer undulations in smectic A have been considered in a variational formulation for rectangular and cylindrical domains (Stewart 1998, Stewart 1999). A short review of smectic layer undulations obtained via the classical Helfrich–Hurault effect may be found in de Gennes and Prost (1993) and Stewart (2004).

When conducting the experiments (Tien 1968, Wobschall 1971, Hopkinson *et al* 2006), the BLMs are reconstituted over solid substrates that possess cylindrical pores. Consequently, they are subjected to hydrostatic pressure perpendicularly to these substrates. To emulate the mechanical behavior of BLMs during these experiments, in the present study the BLMs that occupy the pores of the substrates are modeled as simply supported plates under normal pressure. The BLMs are assumed to be smectic A liquid crystals. The governing equilibrium equations and boundary conditions are derived by using variational methods and the well-known elastic energy discussed by de Gennes and Prost (1993). The series solution is

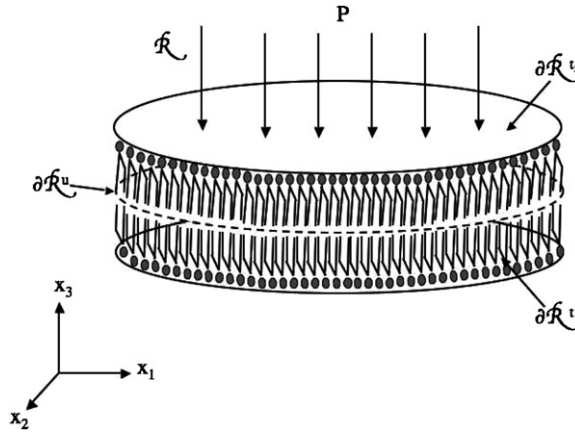


Figure 1. BLM subjected to a uniform constant pressure.

expressed in term of cylindrical functions and proved to be convergent. The deformation of BLMs is illustrated for values of the parameters that are found in the literature.

2. Model formulation

Consider a circular BLM with simply supported edges subjected to a normal pressure (see figure 1). Hereafter, the boundary value problem for the BLM is derived within the theoretical framework for smectic A liquid crystals set forth in de Gennes and Prost (1993) by using variational methods. The resulting linear fourth-order partial differential equation is solved under simplifying assumption on the form of the deflection. By applying the cylindrical functions and their properties, a convergent series solution (given by equation (61) below) is obtained. Finally, the deflection of the BLM is plotted for the values of the parameters reported in the literature.

2.1. Equilibrium equations and boundary conditions

Consider the Cartesian coordinate system with orthonormal basis $\{\mathbf{e}_1, \mathbf{e}_2, \mathbf{e}_3\}$ as shown in figure 1. Let \mathcal{R} denote the volume region occupied by the BLM. Moreover, let $\partial\mathcal{R} = \partial\mathcal{R}^u \cup \partial\mathcal{R}^{t1} \cup \partial\mathcal{R}^{t2}$ be its boundary (see figure 1). Let \mathbf{n} be a unit vector, called the director, which denotes the average alignment of lipid molecules. In a first-order approximation, the vector \mathbf{n} has components (de Gennes and Prost 1993)

$$\mathbf{n} = \left(-\frac{\partial u}{\partial x_1}, -\frac{\partial u}{\partial x_2}, 1 \right), \quad \left| \frac{\partial u}{\partial x_1} \right|, \left| \frac{\partial u}{\partial x_2} \right| \ll 1, \quad (1)$$

where $u = u(x_1, x_2, x_3)$ denotes the layer vertical displacement. If the BLM is assumed not to bend very much from the $x_1 - x_2$ plane and not to strongly compress, the bulk elastic energy density has been shown to have the following form (de Gennes and Prost 1993, p 343)

$$\mathcal{E} = \frac{\bar{B}}{2} \left(\frac{\partial u}{\partial x_3} \right)^2 + \frac{K_1}{2} \left(\frac{\partial^2 u}{\partial x_1^2} + \frac{\partial^2 u}{\partial x_2^2} \right)^2 + 2K_1 \left[\left(\frac{\partial^2 u}{\partial x_1 \partial x_2} \right)^2 - \frac{\partial^2 u}{\partial x_1^2} \frac{\partial^2 u}{\partial x_2^2} \right], \quad (2)$$

where \bar{B} and K_1 are two (positive) constants that have energy length⁻³ and energy length⁻¹ dimensions, respectively, and define the static properties of smectic A liquid crystals. The constant \bar{B} is the smectic layer compression constant and K_1 is the usual Frank splay elastic

constant. In equation (2) above, the usual K_{24} saddle-splay elastic constant has been set equal to $2K_1$: this approximation is in accordance with the *a priori* Ericksen inequalities for the elastic constants (see (Stewart 2004, p 22), noting that K_{24} is equivalent to $K_2 + K_4$). The length $\lambda = (K_1/\bar{B})^{\frac{1}{2}}$ has been found to be comparable to the layer thickness (de Gennes and Prost 1993). In particular, the first term in equation (2) is the compressive-dilatational energy of the layers whereas the other terms account for the saddle-splay energy (de Gennes and Prost 1993). The form of energy density in (2) is also related to the elastic energy density for plates (Landau and Lifshitz 1986, p 39).

The total potential energy that results from the sum of the bulk elastic energy (2) and the pressure, $P = P(r)$, acting normal to the BLM as shown in figure 1, is

$$\mathcal{F} = \int_{\mathcal{R}} \left\{ \frac{\bar{B}}{2} \left(\frac{\partial u}{\partial x_3} \right)^2 + \frac{K_1}{2} \left(\frac{\partial^2 u}{\partial x_1^2} + \frac{\partial^2 u}{\partial x_2^2} \right)^2 + 2K_1 \left[\left(\frac{\partial^2 u}{\partial x_1 \partial x_2} \right)^2 - \frac{\partial^2 u}{\partial x_1^2} \frac{\partial^2 u}{\partial x_2^2} \right] \right\} dV \quad (3)$$

$$+ \int_{\partial \mathcal{R}^2} P u \, dA, \quad (4)$$

with the boundary conditions

$$\mathbf{u} = \mathbf{0} \quad \text{on} \quad \partial \mathcal{R}^u, \quad (5)$$

$$\mathbf{t} = \mathbf{0} \quad \text{on} \quad \partial \mathcal{R}^t, \quad (6)$$

$$\mathbf{t} = -P \mathbf{e}_3 \quad \text{on} \quad \partial \mathcal{R}^t, \quad (7)$$

where $\mathbf{u} = -u(x_1, x_2, x_3)\mathbf{e}_3$ denotes the displacement vector and \mathbf{t} denotes the traction vector. It needs to be emphasized that no torque is applied on the lateral surface of the BLM.

In order to derive *both* the equilibrium equations and the boundary conditions, functional (3) is minimized by using variational methods. Because of the geometrical symmetry of the BLM, cylindrical coordinates, (r, θ, z) , are used to simplify the treatment of the problem. Then, the region \mathcal{R} can be expressed as

$$\mathcal{R} = \{(r, \theta, z) : 0 \leq r \leq b, 0 \leq \theta \leq 2\pi, 0 \leq z \leq h\}, \quad (8)$$

where b and h are the radius and thickness of the BLM, respectively. Moreover, let $\hat{u}(r, \theta, z)$ denote the layer vertical displacement in cylindrical coordinates. It readily follows that functional (3) can be re-written as

$$\begin{aligned} \hat{\mathcal{F}} = & \int_0^{2\pi} \int_0^h \int_0^b \left\{ \frac{\bar{B}}{2} \left(\frac{\partial \hat{u}}{\partial z} \right)^2 + K_1 \left[-\frac{1}{r^2} \frac{\partial^2 \hat{u}}{\partial r^2} \frac{\partial^2 \hat{u}}{\partial \theta^2} + \frac{1}{r^3} \frac{\partial \hat{u}}{\partial r} \frac{\partial^2 \hat{u}}{\partial \theta^2} + \frac{1}{r^4} \left(\frac{\partial^2 \hat{u}}{\partial \theta^2} \right)^2 - \frac{1}{r} \frac{\partial^2 \hat{u}}{\partial r^2} \frac{\partial \hat{u}}{\partial r} \right. \right. \\ & \left. \left. + \frac{1}{2} \left(\frac{\partial^2 \hat{u}}{\partial r^2} \right)^2 + \frac{1}{2r^2} \left(\frac{\partial \hat{u}}{\partial r} \right)^2 - \frac{4}{r^3} \frac{\partial^2 \hat{u}}{\partial r \partial \theta} \frac{\partial \hat{u}}{\partial \theta} + \frac{2}{r^2} \left(\frac{\partial^2 \hat{u}}{\partial r \partial \theta} \right)^2 + \frac{2}{r^4} \left(\frac{\partial \hat{u}}{\partial \theta} \right)^2 \right] \right\} r \, dr \, dz \, d\theta \\ & + \int_0^{2\pi} \int_0^b P \hat{u} r \, dr \, d\theta. \end{aligned} \quad (9)$$

Due to the symmetry of the BLM volume region, the layer vertical displacement can be assumed to be independent of θ , i.e. $\hat{u} = \hat{u}(r, z)$. Under this assumption, functional (9) takes the simplified form

$$\begin{aligned} \hat{\mathcal{F}} = & \int_0^{2\pi} \int_0^h \int_0^b \left[\frac{\bar{B}}{2} \left(\frac{\partial \hat{u}}{\partial z} \right)^2 - \frac{K_1}{r} \frac{\partial^2 \hat{u}}{\partial r^2} \frac{\partial \hat{u}}{\partial r} + \frac{K_1}{2} \left(\frac{\partial^2 \hat{u}}{\partial r^2} \right)^2 + \frac{K_1}{2r^2} \left(\frac{\partial \hat{u}}{\partial r} \right)^2 \right] r \, dr \, dz \, d\theta \\ & + \int_0^{2\pi} \int_0^b P \hat{u} r \, dr \, d\theta, \end{aligned} \quad (10)$$

and, hence, it follows that

$$\hat{\mathcal{F}} = 2\pi \int_0^h \int_0^b \left[\frac{\bar{B}}{2} \left(\frac{\partial \hat{u}}{\partial z} \right)^2 - \frac{K_1}{r} \frac{\partial^2 \hat{u}}{\partial r^2} \frac{\partial \hat{u}}{\partial r} + \frac{K_1}{2} \left(\frac{\partial^2 \hat{u}}{\partial r^2} \right)^2 + \frac{K_1}{2r^2} \left(\frac{\partial \hat{u}}{\partial r} \right)^2 \right] r \, dr \, dz + 2\pi \int_0^b P \hat{u} r \, dr. \tag{11}$$

The boundary conditions (5)–(7) assume the form

$$u(b, z) = 0 \quad 0 \leq z \leq h, \tag{12}$$

$$\frac{\partial u}{\partial z}(r, 0) = 0 \quad 0 \leq r \leq b, \tag{13}$$

$$\frac{\partial u}{\partial z}(r, h) = -\frac{P(r)}{B} \quad 0 \leq r \leq b. \tag{14}$$

The final solution we derive, given by equation (61), can be verified to have a finite energy density at $r = 0$.

Let us consider the variation $\delta \hat{\mathcal{F}}$ of the functional $\hat{\mathcal{F}}$ by assuming that the volume region \mathcal{R} does not change and that $\hat{u}^*(r, z) = \hat{u}(r, z) + \epsilon \psi(r, z) + \dots$, where $\psi = \psi(r, z)$ is a continuous differentiable function and the dots denote terms of order higher than 1 relative to ϵ (Gelfand and Fomin 2000). The variation $\delta \hat{\mathcal{F}}$ of functional (11) is the principal linear part in ϵ of the difference

$$\hat{\mathcal{F}}[\hat{u}^*] - \hat{\mathcal{F}}[\hat{u}]. \tag{15}$$

It needs to be noted that

$$\hat{\mathcal{F}}[\hat{u}^*] - \hat{\mathcal{F}}[\hat{u}] = 2\pi \epsilon \left\{ \int_0^h \int_0^b K_1 \left[\frac{\partial \psi}{\partial r} \left(\frac{1}{r} \frac{\partial \hat{u}}{\partial r} - \frac{\partial^2 \hat{u}}{\partial r^2} \right) + \frac{\partial^2 \psi}{\partial r^2} \left(r \frac{\partial^2 \hat{u}}{\partial r^2} - \frac{\partial \hat{u}}{\partial r} \right) \right] + \bar{B} r \frac{\partial \hat{u}}{\partial z} \frac{\partial \psi}{\partial z} \, dr \, dz + \int_0^b P r \psi \, dr \, dz \right\} + \dots. \tag{16}$$

Since

$$\frac{\partial \hat{u}}{\partial z} \frac{\partial \psi}{\partial z} = \frac{\partial}{\partial z} \left(\frac{\partial \hat{u}}{\partial z} \psi \right) - \frac{\partial^2 \hat{u}}{\partial z^2} \psi, \tag{17}$$

$$\frac{\partial \psi}{\partial r} \left(\frac{1}{r} \frac{\partial \hat{u}}{\partial r} - \frac{\partial^2 \hat{u}}{\partial r^2} \right) = \frac{\partial}{\partial r} \left[\left(\frac{1}{r} \frac{\partial \hat{u}}{\partial r} - \frac{\partial^2 \hat{u}}{\partial r^2} \right) \psi \right] - \psi \left(-\frac{1}{r^2} \frac{\partial \hat{u}}{\partial r} + \frac{1}{r} \frac{\partial^2 \hat{u}}{\partial r^2} - \frac{\partial^3 \hat{u}}{\partial r^3} \right), \tag{18}$$

and, for Green–Riemann’s theorem,

$$\int_0^h \int_0^b \frac{\partial^2 \psi}{\partial r^2} \left(r \frac{\partial^2 \hat{u}}{\partial r^2} - \frac{\partial \hat{u}}{\partial r} \right) \, dr \, dz = \int_0^h \int_0^b \psi \frac{\partial^2}{\partial r^2} \left(r \frac{\partial^2 \hat{u}}{\partial r^2} - \frac{\partial \hat{u}}{\partial r} \right) \, dr \, dz + \oint \frac{\partial \psi}{\partial r} \left(r \frac{\partial^2 \hat{u}}{\partial r^2} - \frac{\partial \hat{u}}{\partial r} \right) - \psi \frac{\partial}{\partial r} \left(r \frac{\partial^2 \hat{u}}{\partial r^2} - \frac{\partial \hat{u}}{\partial r} \right) \, dz, \tag{19}$$

the variation $\delta \hat{\mathcal{F}}$ can be expressed as

$$\delta \hat{\mathcal{F}} = 2\pi \epsilon \left\{ \int_0^h \int_0^b \bar{B} r \frac{\partial}{\partial z} \left(\frac{\partial \hat{u}}{\partial z} \psi \right) + K_1 \frac{\partial}{\partial r} \left[\left(\frac{1}{r} \frac{\partial \hat{u}}{\partial r} - \frac{\partial^2 \hat{u}}{\partial r^2} \right) \psi \right] + \psi \left[K_1 \left(\frac{\partial^4 \hat{u}}{\partial r^4} + \frac{2}{r} \frac{\partial^3 \hat{u}}{\partial r^3} - \frac{1}{r^2} \frac{\partial^2 \hat{u}}{\partial r^2} + \frac{1}{r^3} \frac{\partial \hat{u}}{\partial r} \right) - \bar{B} \frac{\partial^2 \hat{u}}{\partial z^2} \right] r \, dr \, dz + K_1 \oint \left[\frac{\partial \psi}{\partial r} \left(r \frac{\partial^2 \hat{u}}{\partial r^2} - \frac{\partial \hat{u}}{\partial r} \right) - \psi r \frac{\partial^3 \hat{u}}{\partial r^3} \right] \, dz \right\} + \int_0^b P r \psi \, dr. \tag{20}$$

Due to the arbitrariness of $\psi(r, z)$, $\delta\hat{\mathcal{F}} = 0$ implies that the following fourth-order linear partial differential equation needs to be satisfied,

$$\frac{\partial^4 \hat{u}}{\partial r^4} + \frac{2}{r} \frac{\partial^3 \hat{u}}{\partial r^3} - \frac{1}{r^2} \frac{\partial^2 \hat{u}}{\partial r^2} + \frac{1}{r^3} \frac{\partial \hat{u}}{\partial r} = \frac{\bar{B}}{K_1} \frac{\partial^2 \hat{u}}{\partial z^2}, \quad (21)$$

for $0 \leq z \leq h$ and $0 \leq r \leq b$.

By noting that

$$\begin{aligned} & \int_0^b \int_0^h \bar{B} r \frac{\partial}{\partial z} \left(\frac{\partial \hat{u}}{\partial z} \psi \right) dz dr + \int_0^b P r \psi dr \\ &= \int_0^b \left[\left(\bar{B} \frac{\partial \hat{u}}{\partial z} + P \right) \psi(r, h) - \bar{B} \frac{\partial \hat{u}}{\partial z}(r, 0) \psi(r, 0) \right] r dr, \end{aligned} \quad (22)$$

and that $\psi(r, h)$ and $\psi(r, 0)$ are arbitrary, the following boundary conditions are derived:

$$\frac{\partial \hat{u}}{\partial z}(r, 0) = 0, \quad 0 \leq r \leq b, \quad (23)$$

$$\frac{\partial \hat{u}}{\partial z}(r, h) = -\frac{P}{\bar{B}}, \quad 0 \leq r \leq b. \quad (24)$$

Moreover, since $\psi(0, z) = \psi(b, z) = 0$, it follows that

$$\int_0^b \frac{\partial}{\partial r} \left[\left(\frac{1}{r} \frac{\partial \hat{u}}{\partial r} - \frac{\partial^2 \hat{u}}{\partial r^2} \right) \psi \right] dr = 0. \quad (25)$$

In addition,

$$\begin{aligned} & \oint \frac{\partial \psi}{\partial r} \left(r \frac{\partial^2 \hat{u}}{\partial r^2} - \frac{\partial \hat{u}}{\partial r} \right) dz \\ &= \int_0^h \frac{\partial \psi}{\partial r}(b, z) \left(b \frac{\partial^2 \hat{u}}{\partial r^2}(b, z) - \frac{\partial \hat{u}}{\partial r}(b, z) \right) + \frac{\partial \psi}{\partial r}(0, z) \left(\frac{\partial \hat{u}}{\partial r}(0, z) \right) dz, \end{aligned} \quad (26)$$

and because $\frac{\partial \psi}{\partial r}(h, z)$ and $\frac{\partial \psi}{\partial r}(0, z)$ are arbitrary, it follows that

$$b \frac{\partial^2 \hat{u}}{\partial r^2}(b, z) - \frac{\partial \hat{u}}{\partial r}(b, z) = 0, \quad 0 \leq z \leq h, \quad (27)$$

which is the boundary condition for simply supported plates, and

$$\frac{\partial \hat{u}}{\partial r}(0, z) = 0, \quad 0 \leq z \leq h, \quad (28)$$

which is a necessary condition for the layer vertical displacement to have a maximum at the center of the BLM. Finally, due to the fact that $\psi(b, z) = 0$ for $0 \leq z \leq h$,

$$\oint r \psi \frac{\partial^3 \hat{u}}{\partial r^3} dz = \int_0^h b \psi(b, z) \frac{\partial^3 \hat{u}}{\partial r^3}(b, z) dz = 0. \quad (29)$$

It is worth noting that the last term in (2) does not contribute to the derivation of the equilibrium equation (21). For these reasons, it does not appear in the energy density adopted by other investigators (Huang 1986, Nielsen *et al* 1998). In the present study, this term is included into the energy density to *derive* the boundary conditions by following a method used by Timoshenko and Woinowsky-Krieger (1959, p 88–89).

2.2. Series solution of boundary value problem

Consider the partial differential equation

$$\frac{\partial^4 \hat{u}}{\partial r^4} + \frac{2}{r} \frac{\partial^3 \hat{u}}{\partial r^3} - \frac{1}{r^2} \frac{\partial^2 \hat{u}}{\partial r^2} + \frac{1}{r^3} \frac{\partial \hat{u}}{\partial r} = \frac{\bar{B}}{K_1} \frac{\partial^2 \hat{u}}{\partial z^2}, \tag{30}$$

where $0 \leq z \leq h$ and $0 \leq r \leq b$ and the boundary conditions

$$\hat{u}(b, z) = 0, \quad 0 \leq z \leq h, \tag{31}$$

$$b \frac{\partial^2 \hat{u}}{\partial r^2}(b, z) - \frac{\partial \hat{u}}{\partial r}(b, z) = 0, \quad 0 \leq z \leq h, \tag{32}$$

$$\frac{\partial \hat{u}}{\partial z}(r, 0) = 0, \quad 0 \leq r \leq b, \tag{33}$$

$$\frac{\partial \hat{u}}{\partial z}(r, h) = -\frac{P(r)}{\bar{B}}, \quad 0 \leq r \leq b. \tag{34}$$

It is assumed that the solution of (30)–(34) exists as a product of a function of r alone and a function of z alone:

$$\hat{u}(r, z) = R(r)Z(z), \tag{35}$$

and, hence,

$$\frac{1}{R} \left(\frac{d^4 R}{dr^4} + \frac{2}{r} \frac{d^3 R}{dr^3} - \frac{1}{r^2} \frac{d^2 R}{dr^2} + \frac{1}{r^3} \frac{dR}{dr} \right) = \frac{\bar{B}}{K_1} \frac{1}{Z} \frac{d^2 Z}{dz^2} = \chi^4, \tag{36}$$

where χ is the separation constant. Thus, the determination of the solutions of the partial differential equation is reduced to the determination of the solution of two ordinary differential equations,

$$\frac{d^4 R}{dr^4} + \frac{2}{r} \frac{d^3 R}{dr^3} - \frac{1}{r^2} \frac{d^2 R}{dr^2} + \frac{1}{r^3} \frac{dR}{dr} - \chi^4 R = 0, \quad 0 \leq r \leq b \tag{37}$$

$$\frac{d^2 Z}{dz^2} - \chi^4 \frac{K_1}{\bar{B}} Z = 0, \quad 0 \leq z \leq h. \tag{38}$$

The general solution of (37) is

$$R(r) = c_1 J_0(\chi r) + c_2 Y_0(\chi r) + c_3 I_0(\chi r) + c_4 K_0(\chi r), \tag{39}$$

where $c_1, c_2, c_3,$ and c_4 are constants, $J_0(\chi r)$ and $Y_0(\chi r)$ are the Bessel functions of the first and second kinds of order zero, respectively, and $I_0(\chi r)$ and $K_0(\chi r)$ are the modified Bessel functions of the first and second kinds of order zero, respectively. Since the solution needs to be bounded at the center of the BLM, i.e. at $r \rightarrow 0, c_2 = c_4 = 0$. The boundary condition (31) requires that $R(b) = 0$ and, hence,

$$c_1 = -c_3 \frac{I_0(\chi b)}{J_0(\chi b)}, \tag{40}$$

so that

$$R(r) = c_3 \left(I_0(\chi r) - \frac{I_0(\chi b)}{J_0(\chi b)} J_0(\chi r) \right). \tag{41}$$

It follows that boundary condition (32) is given by

$$c_3 \chi^2 b \left(I_2(\chi b) - \frac{I_0(\chi b) J_2(\chi b)}{J_0(\chi b)} \right) = 0. \tag{42}$$

The possibility that $c_3 = 0$ leads to the trivial solution. Thus, in order to find non-trivial solutions of (42), χ is chosen to be a solution of the following equation:

$$J_0(\chi b)I_2(\chi b) - I_0(\chi b)J_2(\chi b) = 0. \quad (43)$$

By writing $x = \chi b$, (43) assumes the form

$$J_0(x)I_2(x) - I_0(x)J_2(x) = 0. \quad (44)$$

Let $x_1 < x_2 < \dots < x_n$ be positive roots of (44). Then, the admissible values of the parameter χ are $\chi_n = \frac{x_n}{b}$.

Next, the general solution of (38) is

$$Z(z) = \frac{d_1}{2} e^{-\chi^2 \sqrt{\frac{K_1}{B}} z} + \frac{d_2}{2} e^{\chi^2 \sqrt{\frac{K_1}{B}} z}, \quad (45)$$

where d_1 and d_2 are constants. From the boundary condition (33), it follows that $d_1 = d_2$. Hence,

$$Z(z) = \frac{d_1}{2} \left(e^{-\chi^2 \sqrt{\frac{K_1}{B}} z} + e^{\chi^2 \sqrt{\frac{K_1}{B}} z} \right) = d_1 \cosh \left(\chi^2 \sqrt{\frac{K_1}{B}} z \right). \quad (46)$$

For convenience, define

$$B_n(r) = J_0(x_n)I_0\left(x_n \frac{r}{b}\right) - I_0(x_n)J_0\left(x_n \frac{r}{b}\right). \quad (47)$$

The set of particular solutions of (30) is

$$\hat{u}_n = d_n B_n(r) \cosh \left(\sqrt{\frac{K_1}{B}} \left(\frac{x_n}{b} \right)^2 z \right), \quad n = 1, 2, \dots \quad (48)$$

By the superposition of these solutions, one obtains the solution

$$\hat{u} = \sum_{n=1}^{\infty} d_n B_n(r) \cosh \left(\sqrt{\frac{K_1}{B}} \left(\frac{x_n}{b} \right)^2 z \right). \quad (49)$$

Suppose that $P = P(r)$ can be expanded as follows:

$$P(r) = \sum_{n=1}^{\infty} c_n B_n(r). \quad (50)$$

Furthermore, assume that $|P(r)| \leq \bar{P}$ for $0 \leq r \leq b$. Multiplying both sides of (50) by $r B_m(r)$ and integrating term by term from 0 to b , one obtains

$$\int_0^b r P(r) B_m(r) dr = \sum_{n=1}^{\infty} c_n \int_0^b r B_n(r) B_m(r) dr. \quad (51)$$

It can be proved (see appendix F) that the sequence of functions

$$\{B_n(r)\} \quad n = 1, 2, \dots \quad (52)$$

has the property that

$$\int_0^b r B_n(r) B_m(r) dr = \begin{cases} 0 & m \neq n, \\ \frac{b^2}{2} (I_0^2(x_n) J_1^2(x_n) - J_0^2(x_n) I_1^2(x_n)) & m = n. \end{cases} \quad (53)$$

Thus, the set of functions $B_n(r)$ for $n = 1, 2, \dots$ is orthogonal with weight r on the interval $[0, b]$. Therefore, the values of the coefficients c_n in (50) are

$$c_n = \frac{\int_0^b P(r) B_n(r) r dr}{\frac{b^2}{2} (I_0^2(x_n) J_1^2(x_n) - J_0^2(x_n) I_1^2(x_n))}. \quad (54)$$

Then, by substituting (49) and (50)–(54) into the boundary condition (34), one obtains

$$\sum_{n=1}^{\infty} d_n \sqrt{\frac{K_1}{B}} \left(\frac{x_n}{b}\right)^2 \sinh\left(\sqrt{\frac{K_1}{B}} \left(\frac{x_n}{b}\right)^2 h\right) B_n(r) = -\frac{1}{B} \sum_{n=1}^{\infty} c_n B_n(r). \quad (55)$$

Consequently, the values of the coefficients d_n in (49) are

$$d_n = -\frac{b^2 c_n}{\sqrt{BK_1} x_n^2 \sinh\left(\sqrt{\frac{K_1}{B}} \left(\frac{x_n}{b}\right)^2 h\right)}, \quad (56)$$

where the coefficients c_n are given by (54).

2.3. Convergence of series solution

Firstly, note that the change of variable $\zeta = r/b$ yields

$$\int_0^b r P(r) B_n(r) dr = b^2 \int_0^1 \zeta P(\zeta b) B_n(\zeta b) d\zeta. \quad (57)$$

Then, by setting

$$A_n(z) = \frac{\cosh\left(\sqrt{\frac{K_1}{B}} \left(\frac{x_n}{b}\right)^2 z\right)}{x_n^2 \sinh\left(\sqrt{\frac{K_1}{B}} \left(\frac{x_n}{b}\right)^2 h\right)}, \quad (58)$$

$$C_n = \int_0^1 P(\zeta b) B_n(\zeta b) \zeta d\zeta, \quad (59)$$

$$D_n = I_0^2(x_n) J_1^2(x_n) - J_0^2(x_n) I_1^2(x_n), \quad (60)$$

the series solution expressed by (49), (54) and (56) can be re-written in a final form suitable for computations as

$$\hat{u}(r, z) = \frac{2b^2}{\sqrt{BK_1}} \sum_{n=1}^{\infty} \frac{C_n}{D_n} A_n(z) B_n(r). \quad (61)$$

It can be seen that

$$|A_n(z)| \leq \frac{1}{x_n^2} \coth\left(\sqrt{\frac{K_1}{B}} \left(\frac{x_n}{b}\right)^2 h\right) \leq \frac{M}{x_n^2}, \quad (62)$$

where $M = \coth\left(\sqrt{\frac{K_1}{B}} \left(\frac{x_1}{b}\right)^2 h\right)$.

For large roots x_n of (44), it is shown in appendices A, E and C, respectively, that

$$|B_n(r)| \leq \frac{2e^{x_n}}{\sqrt{\pi x_n}}, \quad |C_n| \leq \frac{2\bar{P} e^{x_n}}{\pi x_n}, \quad D_n \approx \frac{e^{2x_n}}{\pi^2 x_n^2} \left(1 + O\left(\frac{1}{x_n}\right)\right). \quad (63)$$

Then, by means of (62)–(63),

$$|\hat{u}_n(r, z)| \leq \frac{4M\bar{P}e^{2x_n}}{\pi^{3/2}x_n^{7/2}} \frac{1}{D_n} \approx \frac{4M\bar{P}\sqrt{\pi}}{x_n^{3/2}}. \quad (64)$$

In appendix B, the large roots x_n of (44) are proved to be given approximately by

$$x_n \approx \pi \left(n - \frac{1}{4}\right). \quad (65)$$

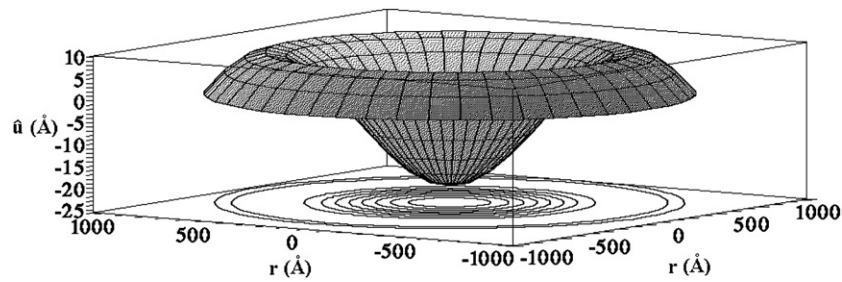


Figure 2. The deflection of a BLM under constant pressure at $z = h$. The deflection $\hat{u}(r, h)$ has been obtained via the solution (61) for values of the parameters reported in table 1.

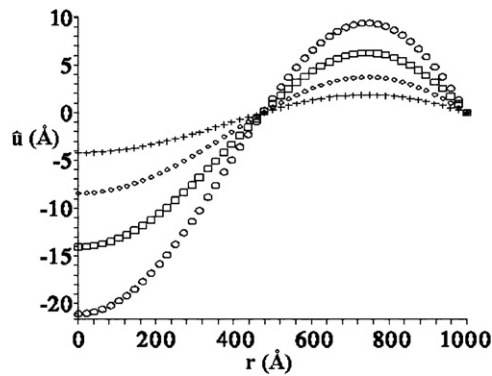


Figure 3. Solution (61) at $z = h$ for $K_1 = 10^{-6}$ (circles), $K_1 = 1.5 \times 10^{-6}$ (squares), $K_1 = 2.5 \times 10^{-6}$ (crosses), and $K_1 = 5 \times 10^{-6}$ (diamonds). The values of h, b, \bar{B}, P are reported in table 1.

Therefore, the inequality (64) with the large roots x_n defined by (65) implies that the series solution (61) is absolutely convergent for $0 \leq r \leq b, 0 \leq z \leq h$.

In figure 2, the surface and the contour plots of the series solution are presented. The series solution (61) has been computed for the values of the material parameters that are reported in table 1. In figures 3 and 4, the solution (61) has been plotted for different values of \bar{B} and K_1 , respectively. In these plots, the other parameters, which also appear in the solution, are fixed to the values reported in table 1. In order to present the results, the pressure $P = P(r)$ has been chosen to be constant. The roots x_n of equation (44) have been computed numerically by implementing Newton's method for small values of n . The numerical process of finding the roots of (44) is then simplified for large values of n . These roots can be approximated by $\pi(n - \frac{1}{4})$.

3. Discussion

A novel mathematical model that describes the pressure effects on the equilibrium configurations of a circular BLM has been presented. The BLM has been assumed to behave as a smectic A liquid crystal. It is subjected to small deformation under pressure loads that are applied perpendicular to the smectic layers. The edges of the biological membrane are assumed to be simply supported. The governing equilibrium equation and boundary conditions are derived by means of variational methods. A series solution of the boundary value problems

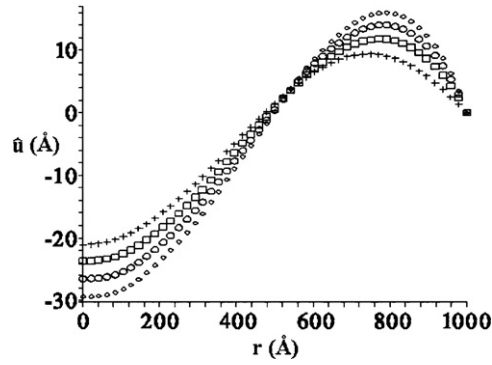


Figure 4. Solution (61) at $z = h$ for $\bar{B} = 10^{-12}$ (diamonds), $\bar{B} = 1.5 \times 10^{-12}$ (circles), $\bar{B} = 3 \times 10^{-12}$ (crosses), and $\bar{B} = 5 \times 10^{-8}$ (squares). The values of h , b , K_1 , P are reported in table 1.

Table 1. Values of parameters.

Parameter	Value	Unit	Reference
K_1 for SOPC	10^{-6}	dyne	(Evans and Rawicz 1990)
\bar{B} for SOPC	5×10^{-8}	dyne \AA^{-2}	(Hladky and Gruen 1982)
h	50	\AA	(Fettiplace <i>et al</i> 1971)
b	1000	\AA	
P	10^{-12}	dyne \AA^{-2}	

has been obtained by employing cylindrical functions. The solution has been proved to be absolutely convergent.

The deflection of the BLM has been numerically computed for values of the parameters that are reported in table 1. As shown in figure 2, the BLM has maximum deflection at its center. It bulges up close to its boundary in the opposite direction of the applied pressure. In figures 3 and 4, it can be observed that the distortion of the BLM decreases as \bar{B} and K_1 decrease. However, the behavior of the solution close to the boundary does not change and, hence, is not determined by the compression and splay-elasticity of the BLM. This behavior is a consequence of the strong anchoring assumption and is an artifact of the model. A replacement of this rather restrictive strong anchoring condition by a more realistic form of weak anchoring is currently being explored by the authors

This theoretical study is motivated by the authors' need of interpreting and synthesize the results of experiments that are currently being conducted at CIMSS (Center for Intelligent Material Systems and Structures), Virginia Tech, to characterize the mechanics of BLMs. Synthetic BLMs of 1-stearoyl-2-oleoyl-3-sn-phosphatidylcholine (SOPC) are reconstituted over hydrophilic polycarbonate membrane with micron or sub-micron pore size. Pressure is applied perpendicular to the BLMs after impedance measurements indicate their formation. The nanometer deformation of the BLM cannot be measured as a function of the applied pressure in this experimental setup. Thus, the findings of this study will be useful in establishing the small deformation that corresponds to a given thickness h of the BLM, applied pressure P and pore radius b of the hydrophilic film.

The values of the saddle splay constant K_1 and compressive constant \bar{B} for BLM of SOPC used in the numerical simulation have been taken from different sources (Hladky and Gruen

1982, Evans and Rawicz 1990). It must be pointed out that to get accurate prediction of the deformation of BLM, tests to determine these constants should have been carried out by using the same experimental settings under the same environmental conditions. Despite these limitations, the results offer some insight on the mechanical response of pressurized BLMs with circular geometry and simply supported edges.

The pressure $P = P(r)$ that acts normal to the lipid layers in the proposed model can be any bounded function of r that admits the representation (50). Therefore, although the numerical simulation and illustrative plots are obtained only for BLMs under uniform pressure loads, the small deformations of the BLMs under different pressure loads such as partial loads and point loads acting on the center of the BLM can be also described by the model.

BLMs are used as platforms to engineer a wide variety of sensors and actuators. Because protein transporters and channels are usually included in these platforms, investigating their influence on the mechanical performance of BLM is crucial for creating viable sensors and actuators. Several investigators have analyzed the effect of lipid bilayers deformation on protein function by accounting for their smectic-A liquid crystalline structure (Huang 1986, Helfrich and Jakobsson 1990, Nielsen *et al* 1998). They have derived mathematical models by using a free energy density that also contains a surface tension contribution. In this study, the BLM surface tension has been assumed to be zero based on arguments presented by Jähnig (1996). Briefly, the attractive interactions between the hydrocarbon tails and the repulsive interactions between the head groups balance each other thus producing an optimal packing of the lipid molecules. The free energy is minimal with respect to the surface area and, hence, the surface tension is zero.

The equilibrium configurations of lipid bilayers have been studied numerically and analytically by using the well-known Helfrich's *spontaneous curvature* model (Helfrich 1973). Unlike the model introduced herein, the earlier model by Helfrich does not include a layer compression term. The retention of a *finite* compression is expected to be more realistic and constitutes one of the defining features of the present study.

For the small distortions considered herein, the molecular axes can be postulated to be normal to the layers. Thus, the director \mathbf{n} and the unit layer normal are assumed to coincide. Future studies will be conducted to describe the deformations of BLMs by accounting for the decoupling of its director \mathbf{n} and the layer unit normal via the recent nonlinear theory of Stewart (2007).

Acknowledgments

This research was supported by the Special Projects Office at DARPA through a NASA contract. R De Vita wishes to thank D J Inman and D J Leo for their hospitality during the course of this study at the Center for Intelligent Material Systems and Structures, Mechanical Engineering Department, Virginia Tech.

Appendix A

Note that $|J_0(x)| \leq 1$ and $I_0(x)$ is monotonically increasing for all x . Thus, one has

$$\begin{aligned} |B_n(r)| &= \left| J_0(x_n) I_0\left(x_n \frac{r}{b}\right) - I_0(x_n) J_0\left(x_n \frac{r}{b}\right) \right| \\ &\leq |J_0(x_n)| \left| I_0\left(x_n \frac{r}{b}\right) \right| + |I_0(x_n)| \left| J_0\left(x_n \frac{r}{b}\right) \right| \\ &\leq 2I_0(x_n) \quad \text{for } 0 \leq r \leq b. \end{aligned} \tag{A.1}$$

For large x , the following asymptotic formula holds, (Rade and Westergren 1999)

$$I_k(x) \approx \frac{e^x}{\sqrt{2\pi x}} \left[1 + O\left(\frac{1}{x}\right) \right] \quad \text{for } k = 0, 1, 2, \dots, \quad (\text{A.2})$$

and, consequently, for large x_n ,

$$I_0(x) \leq \frac{e^{x_n}}{\sqrt{\pi x_n}}. \quad (\text{A.3})$$

Finally, by using (A.3) in (A.1), one finds that

$$|B_n(r)| \leq \frac{2e^{x_n}}{\sqrt{\pi x_n}} \quad \text{for } 0 \leq r \leq b. \quad (\text{A.4})$$

Appendix B

For large x , the asymptotic expressions

$$J_k(x) \approx \sqrt{\frac{2}{\pi x}} \left[\cos\left(x - \frac{\pi}{4} - \frac{k\pi}{2}\right) + O\left(\frac{1}{x}\right) \right] \quad k = 0, 1, 2, \dots, \quad (\text{B.1})$$

are well-known (Rade and Westergren 1999). By using (A.2) and (B.1), it can be easily verified that for large x

$$\begin{aligned} J_0(x)I_2(x) - I_0(x)J_2(x) &\approx \frac{e^x}{\pi x} \left[\cos\left(x - \frac{\pi}{4}\right) - \cos\left(x - \frac{\pi}{4} - \pi\right) + O\left(\frac{1}{x}\right) \right] \\ &= \frac{e^x}{\pi x} \left[2 \cos\left(x - \frac{\pi}{4}\right) + O\left(\frac{1}{x}\right) \right] \\ &= \frac{2e^x}{\pi x} \left[\sin\left(x + \frac{\pi}{4}\right) + O\left(\frac{1}{x}\right) \right]. \end{aligned} \quad (\text{B.2})$$

Thus, the large roots x_n of (44) can be approximated by

$$x_n + \frac{\pi}{4} \approx n\pi \quad (\text{B.3})$$

or, equivalently,

$$x_n \approx \pi \left(n - \frac{1}{4} \right) \quad \text{for large } n. \quad (\text{B.4})$$

Appendix C

From the asymptotic formulas (A.2) and (B.1), it follows that

$$I_m^2(x_n) \approx \frac{e^{2x_n}}{2\pi x_n} \left[1 + O\left(\frac{1}{x_n}\right) \right] \quad \text{for } m = 0, 1, \quad (\text{C.1})$$

$$J_0^2(x_n) \approx \frac{2}{\pi x_n} \cos^2\left(x_n - \frac{\pi}{4}\right) + O\left(\frac{1}{x_n^2}\right), \quad (\text{C.2})$$

$$J_1^2(x_n) \approx \frac{2}{\pi x_n} \cos^2\left(x_n - \frac{\pi}{4} - \frac{\pi}{2}\right) + O\left(\frac{1}{x_n^2}\right), \quad (\text{C.3})$$

and, consequently,

$$\begin{aligned}
 D_n &\approx \frac{e^{2x_n}}{\pi^2 x_n^2} \left[\cos^2 \left(x_n - \frac{\pi}{4} - \frac{\pi}{2} \right) - \cos^2 \left(x_n - \frac{\pi}{4} \right) + O \left(\frac{1}{x_n} \right) \right] \\
 &= \frac{e^{2x_n}}{\pi^2 x_n^2} \left[\sin^2 \left(x_n - \frac{\pi}{4} \right) - \cos^2 \left(x_n - \frac{\pi}{4} \right) + O \left(\frac{1}{x_n} \right) \right] \\
 &= \frac{-e^{2x_n}}{\pi^2 x_n^2} \left[\cos \left(2x_n - \frac{\pi}{2} \right) + O \left(\frac{1}{x_n} \right) \right] \\
 &= \frac{-e^{2x_n}}{\pi^2 x_n^2} \left[\sin(2x_n) + O \left(\frac{1}{x_n} \right) \right].
 \end{aligned} \tag{C.4}$$

Moreover, by means of (B.4), one has that for large x_n

$$\sin(2x_n) \approx \sin \left[2\pi \left(n - \frac{1}{4} \right) \right] = -1. \tag{C.5}$$

Hence,

$$D_n \approx \frac{e^{2x_n}}{\pi^2 x_n^2} \left[1 + O \left(\frac{1}{x_n} \right) \right] \quad \text{for large } x_n. \tag{C.6}$$

Appendix D

Note that the change of variable $\eta = x_n \zeta$ in the following integral leads to

$$\int_0^1 |\zeta P(b\zeta) J_0(x_n \zeta)| d\zeta = \frac{1}{x_n^2} \int_0^{x_n} \left| \eta P \left(b \frac{\eta}{x_n} \right) J_0(\eta) \right| d\eta. \tag{D.1}$$

By Schwartz's inequality and recalling that $|P(r)| \leq \bar{P}$ for $0 \leq r \leq b$, one obtains that

$$\begin{aligned}
 \int_0^{x_n} \left| \eta P \left(b \frac{\eta}{x_n} \right) J_0(\eta) \right| d\eta &\leq \left[\int_0^{x_n} \eta P^2 \left(b \frac{\eta}{x_n} \right) d\eta \right]^{\frac{1}{2}} \left[\int_0^{x_n} \eta J_0^2(\eta) d\eta \right]^{\frac{1}{2}} \\
 &\leq \bar{P} \left[\int_0^{x_n} \eta d\eta \right]^{\frac{1}{2}} \left[\int_0^{x_n} \eta J_0^2(\eta) d\eta \right]^{\frac{1}{2}} = \frac{\bar{P} x_n}{\sqrt{2}} \left[\int_0^{x_n} \eta J_0^2(\eta) d\eta \right]^{\frac{1}{2}}.
 \end{aligned} \tag{D.2}$$

Next, note that (Watson 1995)

$$\int x J_k^2(\alpha x) dx = \frac{x^2}{2} [J_k^2(\alpha x) - J_{k-1}(\alpha x) J_{k+1}(\alpha x)], \tag{D.3}$$

where $k = 0, 1, 2, \dots$ and α is a nonzero real number. Hence, since $J_{-k}(x) = (-1)^k J_k(x)$ for all x with $k = 1, 2, 3, \dots$, from (D.3) it readily follows that

$$\int_0^{x_n} \eta J_0^2(\eta) d\eta = \frac{x_n^2}{2} [J_0^2(x_n) + J_1(x_n) J_2(x_n)]. \tag{D.4}$$

Hence, for large x_n ,

$$\begin{aligned}
 |J_0^2(x_n) + J_1(x_n) J_2(x_n)| &\leq \frac{2}{\pi x_n} \left[\cos^2 \left(x_n - \frac{\pi}{4} \right) \right. \\
 &\quad \left. + \left| \cos \left(x_n - \frac{\pi}{4} - \frac{\pi}{2} \right) \right| \left| \cos \left(x_n - \frac{\pi}{4} - \pi \right) \right| \right] + O \left(\frac{1}{x_n^2} \right) \\
 &\leq \frac{4}{\pi x_n} + O \left(\frac{1}{x_n^2} \right).
 \end{aligned} \tag{D.5}$$

Then,

$$0 \leq \frac{x_n^2}{2} [J_0^2(x_n) + J_1(x_n)J_2(x_n)] \leq \frac{2x_n}{\pi} + O(1), \tag{D.6}$$

and, consequently,

$$\left\{ \frac{x_n^2}{2} [J_0^2(x_n) + J_1(x_n)J_2(x_n)] \right\}^{\frac{1}{2}} \leq \sqrt{\frac{2x_n}{\pi}} + O\left(\frac{1}{x_n^{1/2}}\right). \tag{D.7}$$

By substituting (D.4) into (D.2) and using (D.7), one obtains that

$$\int_0^{x_n} \left| \eta P\left(b\frac{\eta}{x_n}\right) J_0(\eta) \right| d\eta \leq \frac{\bar{P}x_n}{\sqrt{2}} \left(\sqrt{\frac{2x_n}{\pi}} + O\left(\frac{1}{x_n^{1/2}}\right) \right). \tag{D.8}$$

Then, by means of (D.8), (D.1) for large x_n gives

$$\int_0^1 |\zeta P(b\zeta) J_0(x_n\zeta)| d\zeta \leq \frac{\bar{P}}{\sqrt{\pi x_n}} + O\left(\frac{1}{x_n^{3/2}}\right). \tag{D.9}$$

Appendix E

Because $I_0(x)$ is monotonically increasing, $|P(b\zeta)| \leq \bar{P}$ for $0 \leq \zeta \leq 1$, and by using (A.2)–(B.1), one finds that, for large x_n ,

$$\begin{aligned} \left| \int_0^1 \zeta P(b\zeta) J_0(x_n) I_0(x_n\zeta) d\zeta \right| &\leq \bar{P} |J_0(x_n)| |I_0(x_n)| \int_0^1 \zeta d\zeta = \frac{\bar{P}}{2} |J_0(x_n)| |I_0(x_n)| \\ &\approx \frac{\bar{P}e^{x_n}}{2\pi x_n} \left[1 + O\left(\frac{1}{x_n}\right) \right] \left| \cos\left(x_n - \frac{\pi}{4}\right) + O\left(\frac{1}{x_n}\right) \right| \\ &\leq \frac{\bar{P}e^{x_n}}{2\pi x_n} \left[1 + O\left(\frac{1}{x_n}\right) \right]. \end{aligned} \tag{E.1}$$

By employing inequalities (A.3) and (D.9),

$$\begin{aligned} \left| \int_0^1 \zeta P(b\zeta) I_0(x_n) J_0(x_n\zeta) d\zeta \right| &= |I_0(x_n)| \left| \int_0^1 \zeta P(b\zeta) J_0(x_n\zeta) d\zeta \right| \\ &\leq |I_0(x_n)| \int_0^1 |\zeta P(b\zeta) J_0(x_n\zeta)| d\zeta \\ &\leq \frac{\bar{P}e^{x_n}}{\pi x_n} \left[1 + O\left(\frac{1}{x_n}\right) \right]. \end{aligned} \tag{E.2}$$

Hence, for large x_n

$$|C_n| \leq \frac{\bar{P}e^{x_n}}{2\pi x_n} \left[1 + 2 + O\left(\frac{1}{x_n}\right) \right] = \frac{3\bar{P}e^{x_n}}{2\pi x_n} \left[1 + O\left(\frac{1}{x_n}\right) \right]. \tag{E.3}$$

Finally, one obtains that

$$|C_n| \leq \frac{2\bar{P}e^{x_n}}{\pi x_n} \quad \text{for large } x_n. \tag{E.4}$$

Appendix F

The change of variable $r = b\zeta$ in the following integral yields

$$\int_0^b r B_n(r) B_m(r) dr = b^2 \int_0^1 \zeta B_n(b\zeta) B_m(b\zeta) d\zeta, \quad (\text{F.1})$$

with $m \neq n$. Note that (Watson 1995)

$$\int_0^1 \zeta J_0(x_n \zeta) J_0(x_m \zeta) d\zeta = \frac{x_m J_0(x_n) J_1(x_m) - x_n J_0(x_m) J_1(x_n)}{x_m^2 - x_n^2}, \quad (\text{F.2})$$

$$\int_0^1 \zeta I_0(x_n \zeta) I_0(x_m \zeta) d\zeta = \frac{x_m I_0(x_n) I_1(x_m) - x_n I_0(x_m) I_1(x_n)}{x_m^2 - x_n^2}, \quad (\text{F.3})$$

$$\int_0^1 \zeta I_0(x_n \zeta) J_0(x_m \zeta) d\zeta = \frac{x_m J_1(x_m) I_0(x_n) + x_n J_0(x_m) I_1(x_n)}{x_m^2 + x_n^2}. \quad (\text{F.4})$$

After some simple calculations, it readily follows from (F.2)–(F.4) that

$$\begin{aligned} \int_0^1 \zeta B_n(b\zeta) B_m(b\zeta) d\zeta &= \frac{x_m I_0(x_n) J_0(x_n) [I_0(x_m) J_1(x_m) + J_0(x_m) I_1(x_m)]}{x_m^2 - x_n^2} \\ &\quad - \frac{x_n I_0(x_m) J_0(x_m) [I_0(x_n) J_1(x_n) + J_0(x_n) I_1(x_n)]}{x_m^2 - x_n^2} \\ &\quad - \frac{x_m I_0(x_n) J_0(x_n) [I_0(x_m) J_1(x_m) + J_0(x_m) I_1(x_m)]}{x_m^2 + x_n^2} \\ &\quad - \frac{x_n I_0(x_m) J_0(x_m) [I_0(x_n) J_1(x_n) + J_0(x_n) I_1(x_n)]}{x_m^2 + x_n^2}. \end{aligned} \quad (\text{F.5})$$

Next, note that (44) can be re-written as

$$x I_0(x) J_0(x) = I_1(x) J_0(x) + I_0(x) J_1(x), \quad (\text{F.6})$$

by using the identities

$$I_{k+1}(x) = I_{k-1}(x) - \frac{2k}{x} I_k(x), \quad J_{k+1}(x) = \frac{2k}{x} J_k(x) - J_{k-1}(x). \quad (\text{F.7})$$

Thus, the roots x_m and x_n of (44) satisfy the following equations:

$$x_m I_0(x_m) J_0(x_m) = I_0(x_m) J_1(x_m) + I_1(x_m) J_0(x_m), \quad (\text{F.8})$$

$$x_n I_0(x_n) J_0(x_n) = I_0(x_n) J_1(x_n) + I_1(x_n) J_0(x_n). \quad (\text{F.9})$$

By substituting the left hand-sides of (F.8)–(F.9) into (F.5), one finds that

$$\int_0^1 \zeta B_n(b\zeta) B_m(b\zeta) d\zeta = I_0(x_m) I_0(x_n) J_0(x_n) J_0(x_m) - I_0(x_m) I_0(x_n) J_0(x_n) J_0(x_m) = 0 \quad (\text{F.10})$$

and, consequently,

$$\int_0^b r B_n(r) B_m(r) dr = 0 \quad \text{for } m \neq n. \quad (\text{F.11})$$

Therefore, the system $\{B_n(r)\}$ with $n = 1, 2, \dots$ is orthogonal with weight r where $0 \leq r \leq b$.

Again, consider the change of variable $r = b\zeta$ in the following integral

$$\int_0^b B_n^2(r)r \, dr = b^2 \int_0^1 B_n^2(b\zeta)\zeta \, d\zeta. \quad (\text{F.12})$$

Next, from (D.3) and $J_0'(x) = -J_1(x)$,

$$\int_0^1 \zeta J_0^2(x_n\zeta) \, d\zeta = \frac{1}{2}[J_1^2(x_n) + J_0^2(x_n)]. \quad (\text{F.13})$$

Since $I_k(x) = i^{-k}J_k(ix)$ with $k = 1, 2, \dots$, it immediately follows from (F.13) that

$$\int_0^1 \zeta I_0^2(x_n\zeta) \, d\zeta = \frac{1}{2}[I_0^2(x_n) - I_1^2(x_n)]. \quad (\text{F.14})$$

Moreover, by setting $m = n$ into (F.4), one derives

$$\int_0^1 \zeta I_0(x_n\zeta)J_0(x_n\zeta) \, d\zeta = \frac{1}{2x_n}[I_0(x_n)J_1(x_n) + J_0(x_n)I_1(x_n)]. \quad (\text{F.15})$$

Since x_n satisfies (F.6), (F.15) simplifies to

$$\int_0^1 I_0(x_n\zeta)J_0(x_n\zeta)\zeta \, d\zeta = \frac{1}{2}[I_0(x_n)J_0(x_n)]. \quad (\text{F.16})$$

From (F.13), (F.14), (F.16), it follows that

$$\int_0^b B_n^2(r)r \, dr = \frac{b^2}{2}[I_0^2(x_n)J_1^2(x_n) - I_1^2(x_n)J_0^2(x_n)]. \quad (\text{F.17})$$

References

- Alberts B *et al* 2002 *Molecular Biology of the Cell* 4th edn (New York: Garland Publishing)
- Collings P J and Hird M 1997 *Introduction to Liquid Crystals Chemistry and Physics* (London: Taylor and Francis)
- Cremer P S and Yang T 1999 Creating spatially addressed arrays of planar supported fluid phospholipid membranes *J. Am. Chem. Soc.* **121** 8130–1
- de Gennes P G and Prost J 1993 *The Physics of Liquid Crystals (Oxford Science Publications)* 2nd edn (Oxford: Oxford University Press)
- Evans E and Rawicz W 1990 Entropy-driven tension and bending elasticity in condensed fluid membranes *Phys. Rev. Lett.* **64** 2094–7
- Fang Y *et al* 2006 Applications of biomembranes in drug discovery *MRS Bull.* **31** 541–5
- Fettiplace R *et al* 1971 The thickness, composition and structure of some lipid bilayers and natural membranes *J. Membr. Biol.* **5** 277–96
- Gelfand I M and Fomin S V 2000 *Calculus of Variations* (New York: Dover)
- Helfrich W 1973 Elastic properties of lipid bilayers: theory and possible experiments *Z. Naturforsch.* **28** 693–703
- Helfrich W and Jakobsson E 1990 Calculation of deformation energies and conformations in lipid membranes containing gramicidin channels *Biophys. J.* **57** 1075–84
- Hladky S B and Gruen D W R 1982 Thickness fluctuations in black lipid membranes *Biophys. J.* **38** 251–8
- Hopkinson D *et al* 2006 Failure pressure of bilayer lipid membranes *Proc. SPIE (San Diego, CA)*
- Hopkinson D and Leo D J 2007 Evaluating the mechanical integrity of bilayer lipid membranes using a high-precision pressurization system *Proc. SPIE (San Diego, CA)*
- Huang H W 1986 Deformation free energy of bilayer membrane and its effect on gramicidin channel lifetime *Biophys. J.* **50** 1061–70
- Jähnig F 1996 What is the surface tension of a lipid bilayer membrane? *Biophys. J.* **71** 1348–9
- Landau L D and Lifshitz E M 1986 *Theory of Elasticity* vol 7, 3rd edn (Oxford: Pergamon)
- Nielsen C *et al* 1998 Energetics of inclusion-induced bilayer deformations *Biophys. J.* **74** 1966–83
- Rade L and Westergren B 1999 *Mathematics Handbook for Science and Engineering* 4th edn (Berlin: Springer)
- Raviv U *et al* 2005 Cationic liposome-microtubule complexes: pathways to the formation of two state lipid–protein nanotubes with open or closed ends *Proc. Natl Acad. Sci. USA* **102** 11167–72
- Sackmann E 1996 Supported membranes: scientific and practical applications *Science* **271** 43–8

- Stewart I W 1998 Layer undulations in finite samples of smectic-A liquid crystals subjected to uniform pressure and magnetic fields *Phys. Rev. E* **58** 5926–33
- Stewart I W 1999 Layer undulations induced by a magnetic or electric field in concentric cylindrical layers of smectic-A liquid crystals *Phys. Rev. E* **60** 1888–96
- Stewart I W 2004 *The Static and Dynamic Continuum Theory of Liquid Crystals* (London: Taylor and Francis)
- Stewart I W 2007 Dynamic theory for smectic A liquid crystals *Contin. Mech. Thermodyn.* **18** 343–60
- Sundaresan V B and Leo D J 2005 Experimental investigation for chemo-mechanical actuation using biological transport mechanisms *Proc. IMECE (Orlando, FL)*
- Tien T H 1968 Bifacial tension of black lipid membranes *Advances in Chem. Ser.* **84** 104–14
- Timoshenko S P and Woinowsky-Krieger S 1959 *Theory of Plates and Shells* (Cambridge: McGraw-Hill)
- Watson G N 1995 *A Treatise on the Theory of Bessel Functions* (Cambridge: Cambridge University Press)
- Wobschall D 1971 Bilayer membrane elasticity and dynamic response *J. Colloid Interface Sci.* **36** 385–96